The COR1 Inner Coronagraph for STEREO-SECCHI

William T. Thompson[1], Joseph M. Davila[2], Richard R. Fisher[2], Larry E. Orwig[2], John E. Mentzell[2], Samuel E. Hetherington[2], Rebecca J. Derro[2], Robert E. Federline[2], David C. Clark[2], Philip T. Chen[2], June L. Tveekrem[2], Anthony J. Martino[2], Joseph Novello[2], Richard P. Wesenberg[2], O. C. StCyr[3], Nelson L. Reginald[3], Russell A. Howard[4], Kimberly I. Mehalick[5], Michael J. Hersh[5], Miles D. Newman[5], Debbie L. Thomas[5], Gregory Card[6], David Elmore[6]

[1]L3 Com. Analytics Corp., NASA GSFC, Code 682.3, Greenbelt, MD 20770 USA
[2]NASA Goddard Space Flight Center, [3]The Catholic University of America
[4]Naval Research Laboratory, [5]Swales Aerospace
[6]High Altitude Observatory, National Center for Atmospheric Research

ABSTRACT

The Solar Terrestrial Relations Observatory (STEREO) is a pair of identical satellites that will orbit the Sun so as to drift ahead of and behind Earth respectively, to give a stereo view of the Sun. STEREO is currently scheduled for launch in November 2005. One of the instrument packages that will be flown on each of the STEREO spacecrafts is the Sun Earth Connection Coronal and Heliospheric Investigation (SECCHI), which consists of an extreme ultraviolet imager, two coronagraphs, and two side-viewing heliospheric imagers to observe solar coronal mass ejections all the way from the Sun to Earth. We report here on the inner coronagraph, labeled COR1. COR1 is a classic Lyot internally occulting refractive coronagraph, adapted for the first time to be used in space. The field of view is from 1.3 to 4 solar radii. A linear polarizer is used to suppress scattered light, and to extract the polarized brightness signal from the solar corona. The optical scattering performance of the coronagraph was first modeled using both the ASAP and APART numerical modeling codes, and then tested at the Vacuum Tunnel Facility at the National Center for Atmospheric Research in Boulder, Colorado. In this report, we will focus on the COR1 optical design, the predicted optical performance, and the observed performance in the lab. We will also discuss the mechanical and thermal design, and the cleanliness requirements needed to achieve the optical performance.

Keywords: Solar coronagraph, space instrumentation

1. OVERVIEW OF THE STEREO MISSION

Observations by the Solar and Heliospheric Observatory[1] (SOHO) have focused the attention of solar astronomers on the importance of coronal mass ejections (CMEs) for understanding the active solar corona and it's interaction with the geomagnetic environment. The Solar Terrestrial Relations Observatory (STEREO) builds on the success of the SOHO mission by observing the three dimensional nature of CMEs. To achieve this objective, two identical spacecraft will be launched into heliocentric drift orbits, one leading Earth and the other lagging, with separation increasing at ± 22 degrees per year. The primary goal of the mission is to track CMEs from their initiation at the Sun to their impact at Earth's magnetosphere.

The STEREO mission will overcome two problems that currently limit existing instrumentation. First, the CMEs that are directed at Earth are hidden by existing coronagraphs' occulting disks, making it difficult to determine their true size and speed. Second, at the present time there are very few ways to track reliably these phenomena after they have departed the coronagraph's field-of-view.

To address these limitations, the STEREO mission will move coronagraphs off of the Sun-Earth line, allowing reliable detection of the Earth-directed CMEs, including tracking them all the way from the Sun to Earth. Further, the STEREO mission will explore angular separation space to determine which angles produce optimal stereoscopic viewing of the Sun's low corona where CMEs originate.

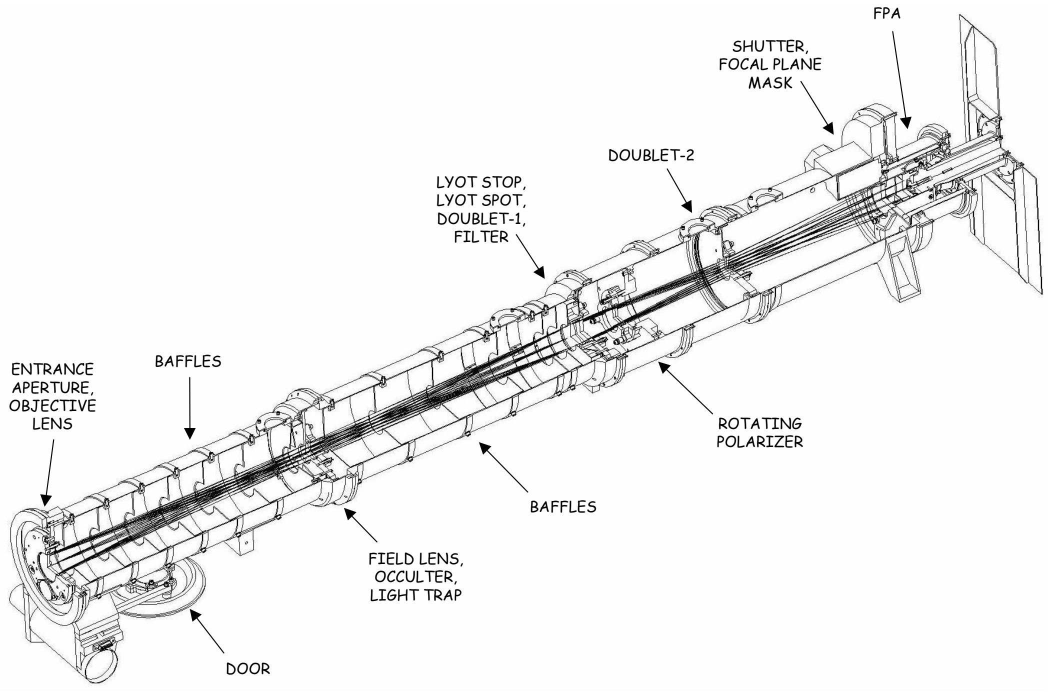

Figure 1. Layout of the COR1 instrument package.

Solar imaging on STEREO will be accomplished with the Sun Earth Connection Coronal and Heliospheric Investigation (SECCHI) instrument package.[2] A series of telescopes are used to image CMEs from the solar surface to the terrestrial environment. The first is an extreme ultraviolet imager (EUVI) that will image the chromosphere and low corona in four emission lines characteristic of coronal temperatures. Two white light coronagraphs extend observations from the EUVI field-of-view out to 15 solar radii. Because of the large gradient in coronal brightness, the inner corona is observed by the COR1 coronagraph, while the outer corona is observed with the COR2 coronagraph. Finally, Earth-directed CMEs are observed from the near-Sun to near-Earth environments by the side-viewing Heliospheric Imager (HI).

We report here on the inner coronagraph, labeled COR1. COR1 is a classic Lyot[3] internally occulting refractive coronagraph, adapted for the first time to be used in space. The field of view is from 1.3 to 4 solar radii. A linear polarizer is used to suppress scattered light, and to extract the polarized brightness signal from the solar corona.

2. OPTICAL LAYOUT

Figure 1 shows the optical layout of the COR1 instrument. Sunlight enters through the front aperture, where the objective lens focuses the solar image onto the occulter. To keep scattering to a minimum, a singlet lens is used for the objective, made of radiation hardened BK7-G18 glass. The primary photosphere light suppression mechanisms in COR-1 are the objective lens to occulter imaging system and the aperture stop to field lens to Lyot stop imaging system. Rather than rely on the on the out of band rejection of the filter, these primary suppression mechanisms are designed to work over the full sensitivity wavelength band of the instrument. The

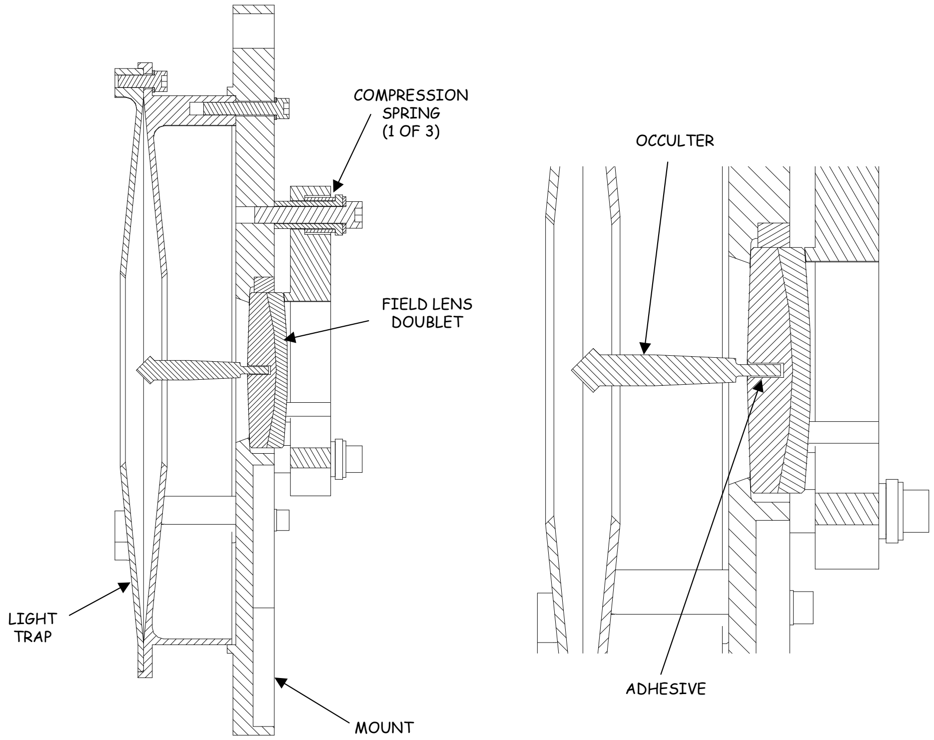

Figure 2. The conical occulter mounted at the center of the field lens, and surrounded by the light trap. Hashed regions show the presence of material at the central plane in this cutaway view.

solar image from the objective will be chromatically aberrated, so the occulter must be sized to block all the solar photospheric light from the near UV to infrared (350–1100 nm). The cut-on at 350 nm is set by the transmission of the BK7-G18 glass in the objective lens, and the cut-off at 1100 nm is set by the band gap of the silicon detector. Subsequent lenses in the optical train balance the chromatic aberration from the objective. The narrow bandpass of the instrument also minimizes the effect of chromatic aberration in the final image.

The occulter is mounted on a stem mounted at the center of the field lens (Figure 2). The tip of the occulter is cone shaped, to direct the sunlight into a light trap which surrounds the occulter. The radius was chosen to block all wavelengths (350–1100 nm) out to a radius of $1.1 R_\odot$. At the design wavelength of 656 nm, the solar image is completely occulted out to 1.30 $R_\odot$, and partially vignetted out to 1.64 $R_\odot$. The wedge-shaped design of the light trap ensures that any ray entering it must reflect many times, so that the light will be absorbed before it can find its way out again.

Diffracted light from the edge of the front aperture is focused onto a Lyot stop and removed. This eliminates the largest source of stray light in the system. Additional stray light rejection is accomplished by placing baffles at various points between the front aperture and Lyot stop. A Lyot spot is also glued to the front surface of the doublet lens immediately behind the Lyot stop, to remove ghosting from the objective lens.

Two doublet lenses are used to focus the coronal image onto the CCD detector. The first, a positive power achromat, is placed immediately behind the Lyot stop, while the second, a negative power acromat, is placed further down the optical path. Together, these act as a telephoto-lens system, focusing the coronal image onto the detector plane, while maintaining diffraction-limited resolution. A bandpass filter 10 nm wide, centered on the Hα line at 656 nm, is placed just behind the first doublet. Thus, the Lyot stop, spot, first doublet, and bandpass filter form a single optical assembly.

A linear polarizer on a hollow core motor rotational stage is located between the two doublets. The current design calls for Corning's Polarcor to be used as the polarizing material, and the placement of the polarizer was chosen to be as close to the first doublet as possible within the dimension constraints of the largest diameter piece of Polarcor that can be obtained (33 mm clear aperture). Normal operations call for three sequential images to be taken with polarizations of 0° and ±60°, to extract the polarized brightness.

A focal plane mask is located between the shutter and the focal plane detector, and is used to remove diffracted light from the edge of the occulter, as discussed below. The detector is an EEV model 42-40 CCD,[2] with 2048 × 2048 pixels, 13.5 μm on a side. Typically, the COR1 images will be 2 × 2 binned onboard before telemetering to the ground. The CCD is backside illuminated, with an anti-reflective coating for high quantum efficiency. A radiator at the back of the instrument ensures low-noise operation by keeping the CCD temperature below -75 °C. The single-pixel full well capacity will be >100,000 electrons, digitized to 14 bits.

3. MECHANICAL AND THERMAL DESIGN

The COR1 mechanical structure is designed as a series of tube sections (Figure 1), which are bolted and pinned together for stability. The individual optics are aligned, mounted, and pinned within these tube sections. COR1 assembly starts from the front tube section, with the objective, occulter, light trap, and field lens, and then each subsequent section is added, together with its associated optical or mechanical components. Because the individual tube sections are pinned together, sections can be taken off and back on again without changing the optical alignment.

Three mechanisms are included in the COR1 instrument package. At the front of the instrument will be a door, to protect the instrument before and during launch, and during spacecraft maneuvers. This door is being supplied by the Max-Planck-Institut für Aeronomie in Lindau, Germany, and is made to the same design as the doors used for the LASCO[4] and EIT[5] instruments on SOHO. On the front of this door will be a diffuser so that the operation of the instrument can be tested when the door is closed, and to provide a flat-field calibration signal.

The other two mechanisms are the hollow core motor to rotate the linear polarizer, and a rotating blade shutter mounted just in front of the focal plane detector assembly, both supplied by Lockheed Martin. All the mechanisms, together with the focal plane CCD detector, will be operated from a centralized control system for all the SECCHI instruments.

Because the two STEREO spacecraft are in elliptical orbits about the Sun, the COR1 instruments will experience considerable variation in solar load, from 1264–1769 and 1068–1482 W/m^2 for the ahead and behind spacecraft respectively. When these loads are combined with the modeled changes in the material thermal properties from beginning to end of life, and with the most extreme differences in the thermal loads from the surrounding structure, the worst-case temperature variation in the COR1 instrument is from 2.5 to 30 °C. There's also an axial gradient in temperature from the front to the back of the instrument, varying from 3 °C in the cold case, to 7 °C in the hot case. Strategically placed software controlled proportional heaters with programmable set points, are used to keep the instrument within the 0–40 °C operational temperature range. There are also survival heaters on mechanical thermostat control to keep the instrument within the -20–55 °C non-operational range.

Specialized composite coatings of oxides over silver are used to help manage the intense solar fluxes which COR1 will be experiencing. The oxide coatings are deposited onto many of the exposed surfaces around the aperture area, such as the objective lens holder assembly and door assemblies, as well as on the front layer of the multilayer insulation. This coating exhibits very low solar absorbtivities, is very stable, and has relatively high IR emissivity values depending on the thickness of the deposited oxide layers.

The majority of the solar load collected by the front objective is concentrated on the occulter tip (Figure 2). In the worst-case analysis, the tip can reach a temperature of 125 °C. This tip is made of titanium, and is diamond turned to direct the sunlight into the light trap. It is coated with a Goddard composite silver coating for high reflectivity. The occulter shaft is coated with black nickel to radiate away the heat. A thin cross-section titanium shaft is used to thermally isolate the occulter from the field lens.

A passive radiator at the back of the spacecraft will be used to maintain the CCD detector at a temperature of about -80 °C. Because this is the side of the spacecraft facing away from the Sun, the radiator will be looking out into empty space. The CCD is conductively isolated by using a thin titanium labyrinth structure to cantilever it off of the main instrument structure. It is radiatively isolated by using multilayer insulation and low emissivity gold coatings on the internal surfaces of the focal plane assembly to minimize parasitic heat into the CCD.

4. STRAY LIGHT MODELING

Two optical analysis codes, APART and ASAP were used to model the expected stray light of the COR1 instrument. While both are products of Breault Research Organization, they are completely independent of each other. ASAP is a Monte-Carlo-based non-sequential raytrace optical code, while APART is a deterministic code developed specifically to analyze the stray light of an optical system. Since this is the first time GSFC has used ASAP for stray light analysis, while APART has been used for years, it was decided to use both codes in a complementary way, to emphasize the strengths of each, while minimizing the weaknesses. We found that the ASAP and APART results agree well with each other, which gives confidence in using ASAP for stray light analysis and shows that the two codes can be used in a complementary fashion to give the most complete and accurate answers possible.

Figure 3 shows the results of the model calculations. The top panel shows the effect of surface roughness alone, for 10 Å, 5 Å, and 3 Å RMS surface microroughness on the objective lens. In order to stay within the 10^{-6} stray light goal to meet the signal-to-noise requirements, a surface roughness of 3 Å or better is needed. When various levels of surface cleanliness are added to the 3 Å microroughness model, the results change dramatically, as shown in the second panel. This demonstrates that a high level of cleanliness is requirement to meet our performance goals. The COR1 cleanliness program is described in Section 7.

5. TESTING AT THE NCAR/HAO FACILITY

Testing was done at the High Altitude Observatory Vacuum Tunnel Facility, which is located at the National Center for Atmospheric Research in Boulder, Colorado (Figure 4). An altitude-azimuth mirror system is used to feed sunlight into one end of a 100 foot evacuated tunnel. Steering signals for the mirrors are provided by a sensor ring within the instrument chamber. A Fresnel lens concentrates the light from the mirrors onto a diffuser window mounted inside the vacuum chamber. The light from the diffuser is then directed down the tunnel axis by a plano-convex lens. An adjustable iris is mounted just past the lens, and forms the target for the instrument chamber at the other end of the tunnel.

A large instrument chamber sits at the other end of the tunnel, within a class 10,000 cleanroom. The tunnel and instrument chamber are evacuated to $\sim$40 μm (0.04 Torr), to remove atmospheric scattering, and to allow the CCD detector to be cooled. The primary cooling was provided by a chilled glycol/water mixture pumped from outside the chamber. A TEC mounted between the CCD and coolant reservoir provided additional cooling and temperature control.

The COR1 breadboards were mounted so that they could be steered in pitch and yaw. They were supported at their center of mass by a cradle arrangement, while the back end was mounted to two crossed linear motion controllers. This allowed precise control of the alignment of the instrument to the source while the chamber was under vacuum.

A photodiode was mounted alongside the front aperture of the breadboard, to monitor the brightness of the source. This photodiode was equiped with a bandpass filter identical to the one incorporated in the breadboard design. Operation and readout of the photodiode was accomplished using a Keithley Model 617 electrometer.

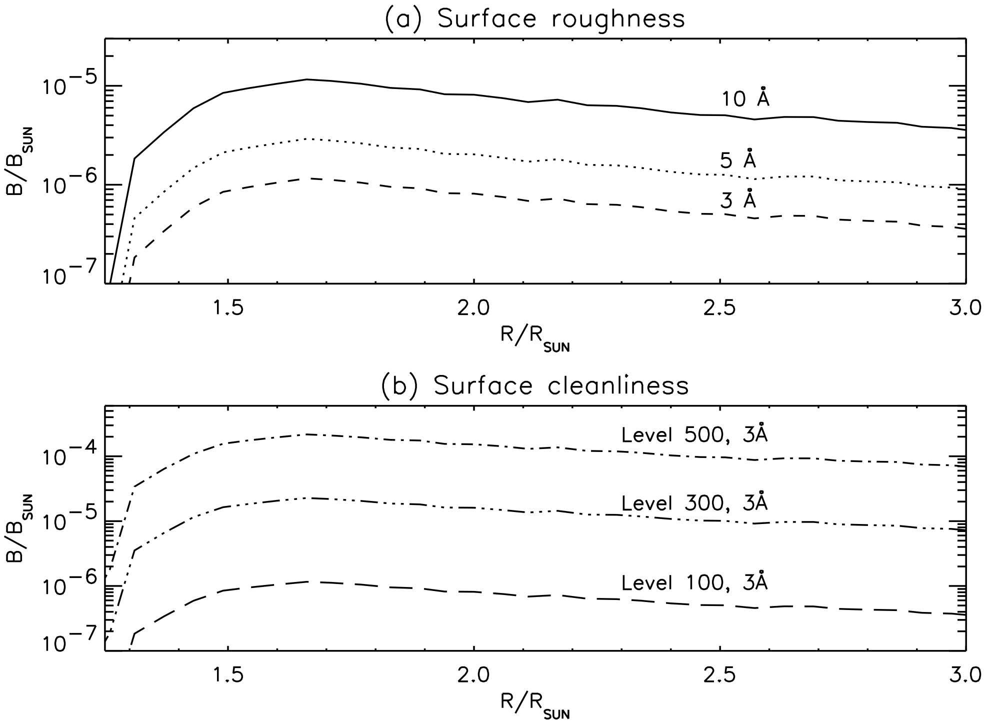

Figure 3. Radially averaged stray light irradiance on the detector at 650 nm, for (a) different levels of RMS surface roughess of a perfectly clean lens, and (b) for different cleanliness levels for a lens with 3 Å RMS surface roughness.

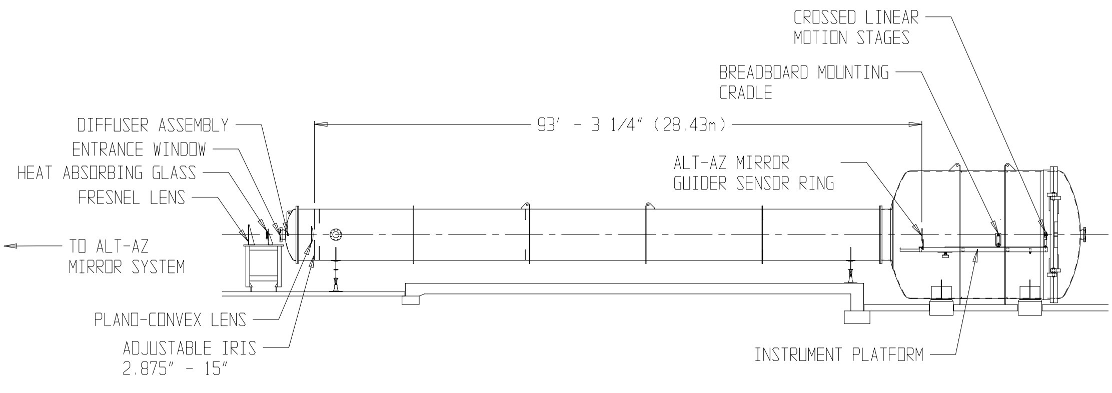

Figure 4. Layout of the NCAR/HAO Vacuum Tunnel Facility.

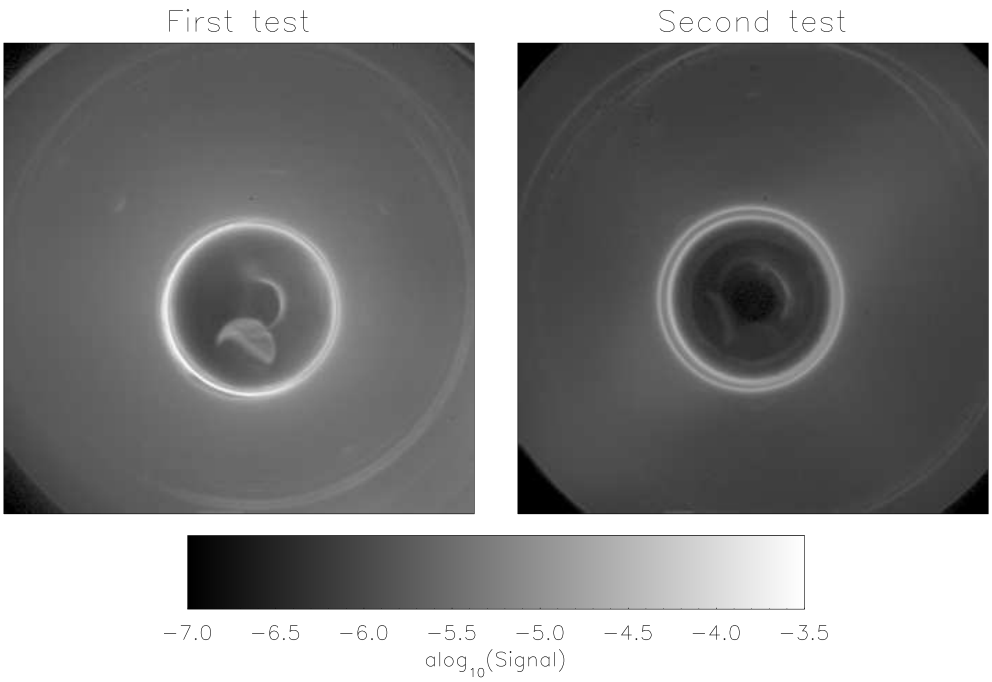

Figure 5. Comparison of the scattered light profile from the two versions of the breadboard.

6. COR1 BREADBOARD RESULTS

Two successive versions of the breadboard were tested, with increasing fidelity to the flight design. The first version used commercial mounts for all the optical elements. It also used an earlier 45° flat occulter design instead of the final conical occulter. The second version introduced a flight-like tube section containing the objective lens, occulter, and field lens, with flight-like lens mounts and baffling, a conical occulter and the corresponding light trap. Both breadboards were designed for a source at a finite 100 foot distance, rather than at infinity.

Significant improvement was seen between the first and second breadboards (Figure 5). The primary cause of this improvement is probably the introduction of better handling procedures for the objective lens. This will be a critical issue for the flight instruments—a dedicated clean room facility has been built for the COR1 instrument assembly, which was not available for the breadboard models. Additional stray light improvement can also be attributed to the introduction of flight-like baffles between the objective and field lens. The change of the occulter design also made a difference, particularly in the bright ring seen around the edge of the occulter. Additional improvement was realized by adding a Lyot spot (Figure 6). The best performance in the final breadboard configuration goes from 10^{-6} $B_{\odot}$ near the edge of the occulter to 2×10^{-7} $B_{\odot}$ at the edge of the detector (∼4 $R_{\odot}$), as demonstrated in Figure 7.

Two bright rings appear around the edge of the occulter. We spent some time after the HAO tests characterizing these rings, and found that both rings are associated with the occulter. One follows the edge of the umbra and the other the edge of the penumbra of the occulter shadow. When the occulter is in perfect focus, the two rings merge into a single ring right at the edge of the occulter. We interpret these rings as diffraction effects occuring at the edge of the occulter, and tied to the diffraction from the aperture. Similar rings have been found in studies of occulters for stellar coronagraphs.[6,7] A focal plane mask will be introduced into the optical path just in front of the detector to remove these two rings.

Two sets of bars radiate from the source image at ±45°, with one set much stronger than the other. By

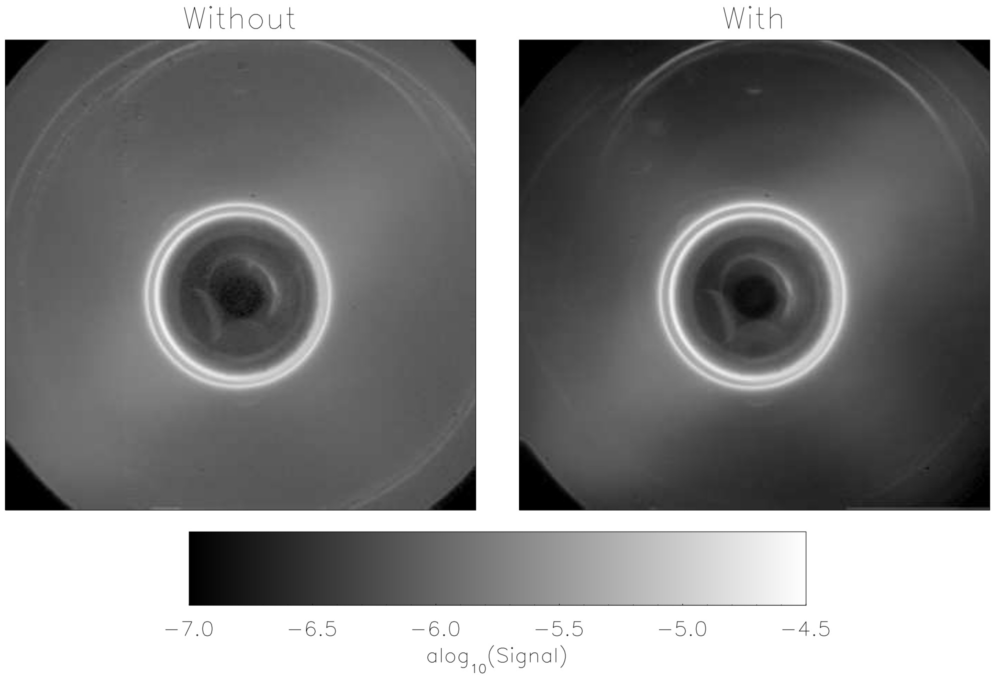

Figure 6. Comparison of the scattered light profile from the second breadboard, with and without a Lyot stop. The image on the left is the same as the right hand image in Figure 5, using a different color table.

changing the pointing of the instrument relative to the source, it was found that these bars are centered on the source rather than on any feature of the instrument. The most likely source is scattering from the objective lens.

There are several artifacts appearing inside the occulter shadow. These have been traced to light hitting a chamfer in the field lens at the end of the occulter stem. In the flight design, the stem will not go all the way through the field lens, so there will not be a chamfer to be illuminated.

The anticipated performance is demonstrated in Figure 8. The measured straylight properties of the breadboard is lower than the model calculations. The data shown in Figure 8 reflect the raw measurements in a single polarizer position. For a single exposure, the scattered light component will always be larger than the K corona. Only after the three polarizer measurements are combined can the underlying polarized brightness signal from the K corona be extracted. Also shown in Figure 8 is the signal-to-noise ratio that can be expected for the polarized brightness signal from the background corona. It should be emphasized that the instrument is designed to observe coronal mass ejections, which will be brighter than the background corona at the higher heights above the solar limb.

7. CLEANLINESS CONTROL

The COR1 instrument is sensitive to light scattering induced by particulate contamination along the optical path. The measurements of the COR1 breadboard models have clearly demonstrated that the cleanliness of the optical surfaces, and particularly the objective lens, is critical to keep the scattered light levels down to acceptable levels. Therefore, COR1 optical surfaces will be verified to level 200 per MIL-STD-1246[9] and maintained at that level through integration and testing (I&T). Additionally, COR1 has a capability of changing out the objective lens just prior to launch, if needed. This will be achieved by pre-aligning and pinning a spare objective lens assembly, which can be switched with the original objective lens assembly.

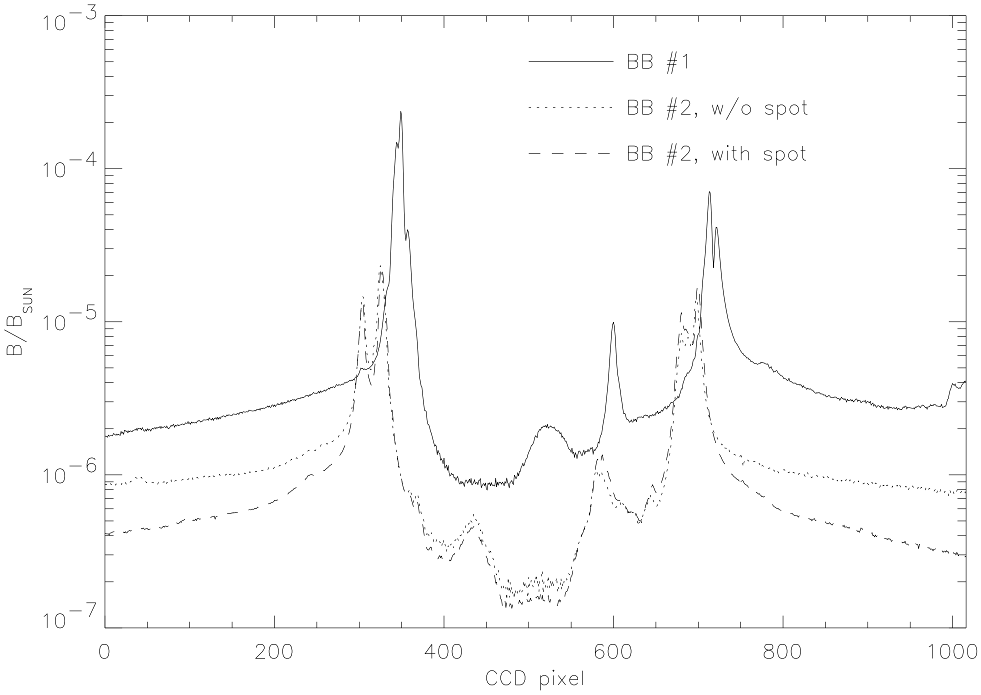

Figure 7. Horizontal traces through the approximate centers of the occulter shadows for breadboard #1 (solid), breadboard #2 without the Lyot spot (dotted), and with the Lyot spot (dashed). The full range of this plot is approximately $8R_\odot$

To preserve COR1 performance, surface contamination levels must be strictly controlled. The levels can be met by conducting COR1 integration and testing in controlled clean areas. Final COR1 testing at NASA/GSFC will be performed inside a Class M3.5 (Class 100) clean tent which is resided in a Class M5.5 (Class 10,000) cleanroom per FED-STD-209.[10] In addition, the COR1 instrument will be purged with high purity (> 99.999%) gaseous nitrogen during all I&T operations, transportation, and at launch site. Other contamination control provisions will be implemented in order to achieve COR1 cleanliness control.

8. FUTURE PLANS

An Engineering Test Unit (ETU) is currently under development, in preparation for building the final flight units. Two configurations are planned for the ETU. One configuration, for vibration testing, will be a complete instrument built to the flight design, but with simulated mechanisms and detector. Some of the optics will also be simulated. The second configuration, for performance testing, will retain the first two tube sections from the first, which will have flight-like optics installed, up to the bandpass filter (see Figure 1). The remaining optics will be mounted on commercial mounts as in the two breadboards.

The ETU will encompass a number of significant improvements over the previous breadboard models. Of most importance is that the ETU assembly will be performed using flight-like procedures in the higher quality cleanroom that will be used for the flight instruments. Also, in the breadboard, a single doublet was used to focus the image onto the detector. This will be replaced by the two-doublet telephoto flight design, which will improve the resolution to flight standards. A polarizer will be inserted into the optical path, to characterize the residual polarization properties of the instrument. Finally, the focal plane mask concept will be tested.

The design of the two final flight units will be based on the ETU design, reiterated to take the results of the ETU tests into account. The two flight units will be identical in all respects except one. Because the two

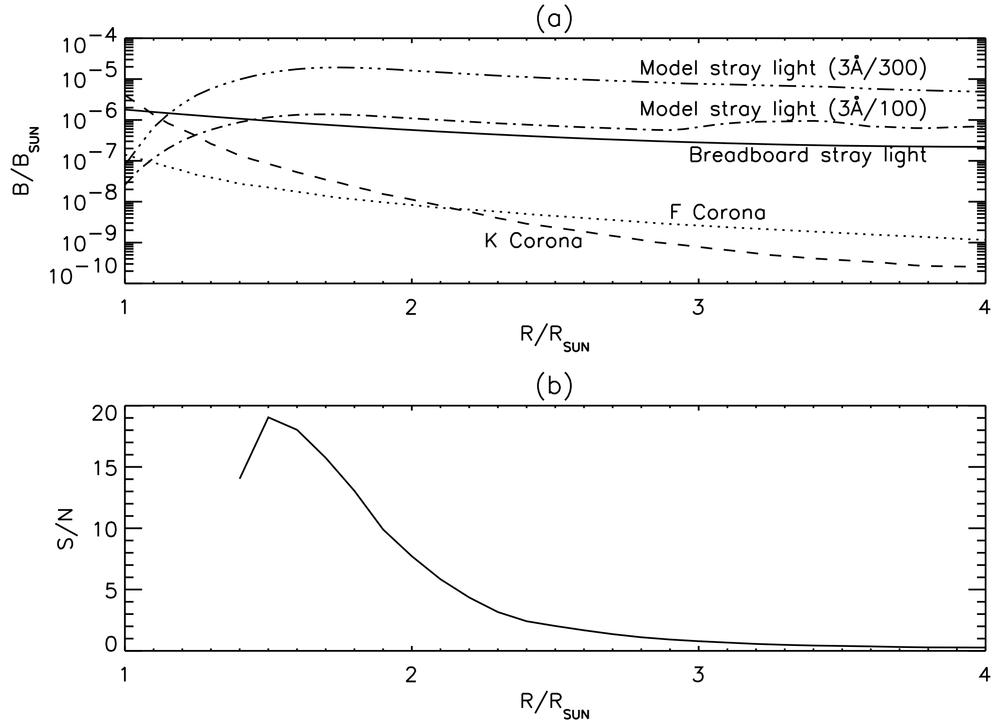

Figure 8. (a) Comparison of the modeled and measured instrumental scattered light to the anticipated background F and K coronae.[8] The curve shown for the breadboard stray light has been extrapolated, and does not include the vignetting from the occulter and focal plane mask. (b) Calculated signal-to-noise ratio for the anticipated background K corona, with vignetting included. When coronal mass ejections move through the field of view, higher signal-to-noise values will be seen.

STEREO spacecraft have slightly different orbits, the ahead spacecraft approaches somewhat closer to the Sun at perihelion than the behind spacecraft. Thus, the solar image will be corresponding larger in the first than the second. This difference will be reflected by having different occulter diameters for the two spacecraft, so that the solar disk will be occulted out to 1.3 $R_\odot$ on each. The diameter of the focal plane mask will also reflect the occulter diameter on each. This is the only difference in the COR1 design between the two spacecraft.

9. CALIBRATING THE FLIGHT INSTRUMENTS

A number of instrument parameters must be considered when calibrating the COR1 flight instruments. The calibration plan should answer the questions: What levels of scattered light are expected? What are the polarization properties of the instrument? What is the instrument flat-field and absolute calibration? What is the spatial resolution?

The COR1 flight models will be calibrated before flight at a vacuum tunnel facility at the Naval Research Laboratory. This is the same facility that was used for calibrating the LASCO coronagraphs on SOHO. The optical setup is similar to that at the NCAR/HAO facility used for the preliminary COR1 breadboard and engineering test models: a simulated solar target is situated down a long evacuated tunnel. Other optical setups will also be used for testing resolution and polarization sensitivity.

Calibration will be done in flight by observing stars and planets. We will also cross-calibrate the overlapping field with COR2. During the early mission phases, we will also be able to cross-calibrate with the Mauna Loa Solar Observatory Mk4 Coronameter.[11,12]

A diffuser window will be mounted in the door, to monitor the instrument calibration and flat-field during flight. This can also be used on the ground for monitoring the alignment of the occulter and focal plane mask.

The baseline design is a 1.0D neutral density filter mounted in front of a pot opal glass diffuser to cut the solar illumination down to $10^{-6}B_{\odot}$, and to distribute the light evenly over the field-of-view. Candidate diffuser configurations are currently being tested.

LEDs of several colors will be included within the focal plane package. These LEDs will be able to stimulate the CCD while the shutter is closed, providing both a liveness test, and a flat-fielding capability for the detector. The different colors give some diagnostics of the CCD during flight.

REFERENCES

1. V. Domingo, B. Fleck, and A. I. Poland, "The SOHO Mission: an Overview," *Solar Phys.* **162**, pp. 1–37, 1995.
2. R. A. Howard, J. D. Moses, and D. G. Socker, "Sun-Earth Connection Coronal and Heliospheric Investigation (SECCHI)," in *Instrumentation for UV/EUV Astronomy and Solar Missions*, *Proc. SPIE* **4139**, pp. 259–283, 2000.
3. B. Lyot, "The study of the solar corona and prominences without eclipses (George Darwin Lecture, 1939)," *Mon. Not. Royal Astron. Soc.* **99**, pp. 580–594, 1939.
4. G. E. Brueckner, R. A. Howard, M. J. Koomen, C. M. Korendyke, D. J. Michels, J. D. Moses, D. G. Socker, K. P. Dere, P. L. Lamy, A. Llebaria, M. V. Bout, R. Schwenn, G. M. Simnett, D. K. Bedford, and C. J. Eyles, "The Large Angle Spectroscopic Coronagraph (LASCO)," *Solar Phys.* **162**, pp. 357–402, 1995.
5. J.-P. Delaboudinière, G. E. Artzner, J. Brunaud, A. H. Gabriel, J. F. Hochedez, F. Millier, X. Y. Song, B. Au, K. P. Dere, R. A. Howard, R. Kreplin, D. J. Michels, J. D. Moses, J. M. Defise, C. Jamar, P. Rochus, J. P. Chauvineau, J. P. Marioge, R. C. Catura, J. R. Lemen, L. Shing, R. A. Stern, J. B. Gurman, W. M. Neupert, A. Maucherat, F. Clette, P. Cugnon, and E. L. van Dessel, "EIT: Extreme-ultraviolet Imaging Telescope for the SOHO mission," *Solar Phys.* **162**, pp. 291–312, 1995.
6. R. J. Terrile and C. Ftaclas, "Application of super smooth optics to extra-solar planet detection," in *Reflective Optics II*, *Proc. SPIE* **1113**, pp. 50–55, 1989.
7. T. Nakajima, "Planet detectability by an adaptive optics stellar coronagraph," *Astrophys. J.* **425**, pp. 348–357, 1994.
8. E. G. Gibson, *The Quiet Sun*, SP-303, National Aeronautics and Space Administration, 1973.
9. MIL-STD-1246C, *Product Cleanliness Levels and Contamination Control Program*, April 1994.
10. FED-STD-209E, *Airborne Particulate Cleanliness Classes in Cleanrooms and Clean Zones*, Sept. 1999.
11. R. R. Fisher, R. H. Lee, R. M. MacQueen, and A. I. Poland, "New Mauna Loa coronagraph systems," *Applied Optics* **20**, pp. 1094–1101, 1981.
12. D. F. Elmore, J. T. Burkepile, J. A. Darnell, A. R. Lecinski, and A. L. Stanger, "Calibration of a ground-based solar coronal polarimeter," in *Polarimetry in Astronomy*, *Proc. SPIE* **4843**, 2002. in press.